

Fig. 1 — A multiaxial spot weld specimen in principle (Ref. 1).

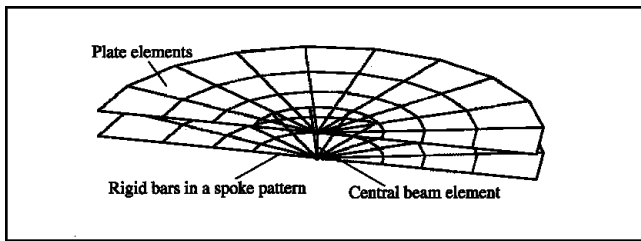


Fig. 3 — Modeling of a spot weld.

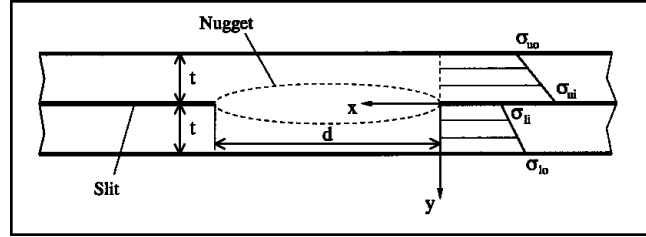


Fig. 2 — Structural stresses around a spot weld.

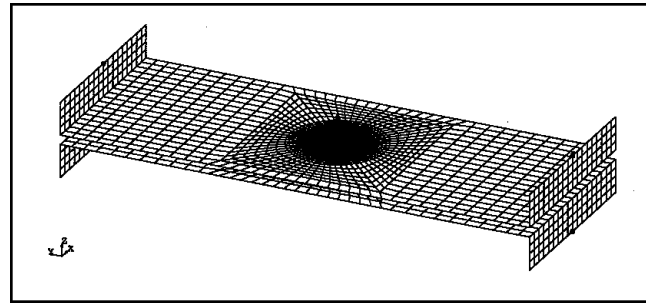


Fig. 4 — Finite element model of the specimen.

Finite Element Validation

The stress formulas derived in the last section cannot be checked by experiments because there is no experimental method available to measure structural stress, notch stress and stress-intensity factors at a spot weld. Finite element simulations are, instead, conducted to validate the formulas. If structural stresses σ_{ui} , σ_{uo} , σ_{li} and σ_{lo} around a spot weld (Fig. 2) are available, structural stress σ_r at the spot weld is directly given by the larger of σ_{ui} and σ_{li} . Notch stress σ_k , and stress-intensity factors K_I and K_{II} at the spot weld can also be determined by the structural stresses around the spot weld (Refs. 2-5). The corresponding equations are listed as follows:

$$\sigma_k = \max\{\sigma_{ui}, \sigma_{li}\} \quad (10)$$

$$\sigma_k = \sigma_n + \frac{1}{4\sqrt{3\pi}} \sqrt{\frac{t}{\rho}}$$

$$\sigma_{ui} - \sigma_{uo} + \sigma_{li} - \sigma_{lo} \pm$$

$$2(\sigma_{ui} - \sigma_{li})^2 + (\sigma_{uo} + \sigma_{lo})^2 \quad 1/2$$

$$\sigma_{ui}^2 + \sigma_{li}^2 - \sigma_{ui}\sigma_{uo}$$

$$+ 2\sigma_{ui}\sigma_{lo} - \sigma_{uo}\sigma_{li}$$

$$- \sigma_{li}\sigma_{lo} \quad (11)$$

$$K_I = \frac{\sqrt{3}}{12} (\sigma_{ui} - \sigma_{uo} + \sigma_{li} - \sigma_{lo}) \sqrt{t} \quad (12)$$

$$K_{II} = \frac{1}{4} (\sigma_{ui} - \sigma_{li}) \sqrt{t} \quad (13)$$

where $n = \sigma_{ui} - \sigma_{li} / (\sigma_{ui} - \sigma_{uo} + \sigma_{li} - \sigma_{lo})$ if $(\sigma_{ui} - \sigma_{li}) / (\sigma_{ui} - \sigma_{uo} + \sigma_{li} - \sigma_{lo}) > 0$ and $n = \sigma_{li} - \sigma_{lo} / (\sigma_{ui} - \sigma_{uo} + \sigma_{li} - \sigma_{lo})$ if $(\sigma_{ui} - \sigma_{li}) / (\sigma_{ui} - \sigma_{uo} + \sigma_{li} - \sigma_{lo}) < 0$. The combined sign \pm in Equation 11 takes the plus if $\sigma_{ui} - \sigma_{uo} + \sigma_{li} - \sigma_{lo} > 0$ and otherwise the minus. As seen from the above equations, the main task for getting the local stress parameters at the spot weld is to determine the structural stresses around the spot weld. To obtain the structural stresses reliably, the spot weld is particularly modeled by a spoke pattern (Ref. 4). The pattern is shown in principle in Fig. 3. The central beam in the spoke pattern is actually a cylindrical bar element with a diameter of the nugget diameter. The diameter of the pattern is also equal to the nugget diameter. Heavy mesh refinements (much finer than that shown in Fig. 3) are introduced around the spoke pattern in order to obtain the structural stresses accurately. The finite element model for the specimen is shown in Fig. 4.

The specimen is loaded at different angles of $\theta = 0, 30, 60$ and 90 deg to cover the whole loading range from shear to tension. The simulations are conducted at two nugget diameters of $d = 5.4$ and 8.0 mm and at two specimen lengths of $b = 79.6$ and 49.6 mm, while the other

Table 1 — Correction Factor η with $e = (w - d)/2$

e/d	1.0	1.5	2.0	2.5	3.0
	1.68	1.47	1.26	1.06	0.94

dimensions of the specimen are kept constant at $w = 31.0$, $t = 1.6$ and $d = 0.2$ mm. The notch root radius $\rho = 0.2$ mm correspond to ferritic steels (Ref. 6). What matters is actually the ratio of the different geometric parameters. The variation of d and b results in significant variations in all the ratios such as d/t , w/d and b/w . Therefore, the finite element simulations are representative for the specimen. The correction factor, interpolated from Table 1, takes different values as well, i.e., $\eta = 1.11$ at $d = 5.4$ mm and $\eta = 1.50$ at $d = 8.0$ mm. Young's modulus of $E = 210,000$ MPa and Poisson's ratio of $\nu = 0.3$ for common steels are generally introduced for all the variants.

On the one hand, the structural stress, notch stress and equivalent stress-intensity factor at the spot weld in the specimen are determined by finite element analyses and Equations 10-13 and 8. On the other hand, they are predicted by the formulas 4, 3 and 9, respectively. The results for all the variants are compared in Tables 2 through 5. As seen from the tables, the values predicted by the stress formulas agree well with those from the fi-

